



Nassira CHERIET ^{1,3}, Mohamed Lamine BENLEKKAM ^{1,2},
Sahraoui KHERRIS ^{1,3}

Influence of fin shape design on thermal efficiency of phase change material-based thermal energy storage unit

Received 18 February 2024, Revised 23 April 2024, Accepted 2 May 2024, Published online 30 May 2024

Keywords: heat storage, PCM, fins shape, melting process, heat exchanger, surface area

The present numerical study is concerned with the impact of fin shape design on the thermal efficiency of phase change material (PCM)-based thermal energy storage (TES) unit, assuming the same surface area occupied by fins. Comparison of two different finned TES units equipped with rectangular and triangular fin shapes, respectively, showed significant enhancements in PCM melting activity. Comparative analysis demonstrated that triangular fin shape lowers PCM melting time by 12.64% for equivalent fin numbers, and by 15.38% for equal fin lengths due to the increased heat transfer area provided by the triangular shape. Further examination of fins with triangular shape in terms of spacing and length, under fixed thickness and size parameters, revealed significant reduction in melting time with increasing fins length. Notably, a 50.75% decrease in melting time was achieved by decreasing the number of fins to 20 while increasing fin length to 10 mm. Moreover, maintaining heat transfer fluid (HTF) temperature 20 K higher than the melting PCM temperature maximizes TES thermal efficiency. These outcomes emphasize the importance of optimizing fin shape design for enhancing heat transfer without affecting the energy storage capacity of TES systems, with potential applications in thermal management systems.

1. Introduction

In the last decades, the use of fossil fuels as a source of energy affects the environment and creates an imbalance in energy demand. It is a major catalyst for

✉ Mohamed Lamine BENLEKKAM, e-mail: benlekkam.mohamed@univ-tissemsilt.dz

¹Tissemsilt University, Faculty of Sciences and Technology, Tissemsilt, Algeria

²Laboratory of Smart Structure, University of AinTemouchent, AinTemouchent, Algeria

³Mechanical Engineering, Materials and Structures Laboratory, Tissemsilt, Algeria



hastening the shift towards more sustainable energy sources. Solar energy represents a huge and a safe source of energy that can be a good alternative. Since solar energy is intermittent, energy storage is necessary to ensure the continuity and provide the energy consumption equilibrium [1]. The latent heat thermal energy storage (LHTES) is the most frequently used technology investigated by the scientific community to provide the necessary heat power. This technology for (PCMs) provides high TES capacity in small volumes at a constant temperature [2, 3].

In fact, PCMs are characterized by their poor thermal conductivity, which affects the LHTES system performance and the power of charge/discharge rates [4]. To overcome this challenge, numerous studies were performed to raise the heat exchange in LHTES, including the utilization of extended fins [5–8] porous metals [9, 10] nanomaterials [11–13] and expanded graphite [14, 15].

Joshi et al. [16] carried out an experimental and numerical evaluation, comparing the melting efficiency of PCM infused with fins against another with metal foam within a rectangular container. Results revealed that with an equal quantity of PCM, fins demonstrated the highest heat transfer efficacy, resulting in a 66.67% faster melting time compared to metal foam. Masoumi et al. [17] examined a LHTES container with and without upstanding fins filled by NePCMs. They discovered that incorporating fins can lower both melting and solidification durations by approximately 54% and 76%, respectively. Nevertheless, it was noted that the utilization of nanoparticles positively impacts the dissolution rate solely in scenarios where the system does not feature fins. The study also highlighted the close relationship between heat flux and both thermal transmission and natural convection. The presence of nanoparticles leads to a simultaneous rise in both the heat transmission and viscosity of the PCM, while increased viscosity particularly hinders the natural convection process.

As mentioned above, the fins are the most widely used technology to enhance heat transmission because of its excellent heat transfer improvement, reduced price, simple design, and ease of manufacturing [14]. Tang et al. [18] assessed the thermal efficiency of horizontal TES unit employing various types of fin configurations, angles, and lengths. The outcomes indicated that the heat efficiency of the LHTES system can be boosted by utilizing a variable fin design with fin lengths lower than the radius of the shell and placed in a region far from the HTF inlet. Additionally, during the melting process, Kazemi et al. [19] and Mahood et al. [20] evaluated the best design of fin angles. They discovered that concentrating the fins toward the bottom half of the container is more impactful on minimizing the melting duration when the unit is positioned transversely due to natural convection. Mudhafar et al. [21] numerically assessed the PCM solidification operation, utilizing three configuration types of heat exchanger: triple tube, webbed tube, and a modified webbed tube. The results revealed that employing the modified webbed tube speeds up the PCM solidification rate by 41%. Bouhal et al. [22] performed a numerical assessment of the gallium melting operation using the enthalpy-porosity approach. Two configurations were assessed: one featuring cylindrical heating el-

ements and the other incorporating four slender fins positioned around the circle of heating elements. The inclusion of fins in the multi-tube setup improves the thermal transmission efficiency and minimizes the required melting interval for the PCM decreasing it from 18,35 minutes to 13,35 minutes.

In fact, some researchers studied addition of a more complicated fin shape to the simplest ones. Zheng et al. [23] conducted a numerical study on various tree-shaped fin designs, ranging from two to four levels of branching. In comparison to a TES system featuring standard straight fins, the four-level tree-shaped fins enhance efficiency by 53% and facilitate a quicker and more consistent solidification process. Zhao et al. [24] numerically examined six variations of the energy storage tank based on various fin designs. The optimized fin design improved heat transfer and decreased melting and solidification periods by 70% and 81%, respectively. Based on the optimization approach, the configuration of fins offered an important advantage, such as metal savings through fewer fins and a smaller weight. Sciacovelli et al. [5] utilized a computational model to examine the impact of single and double Y-shaped fin bifurcation on TES efficiency. According to their findings, the use of fins can significantly rise the TES effectiveness. Moreover, a smaller angle of the Y-shaped fins is required for long operating times. Pizzolato et al. [25, 26] presented topology optimization of fin designs for LHTES units. The outcomes indicated that the novel fins configuration could significantly enhance the thermal transmission effectiveness. Tian et al. [27] developed a computational model to optimize the bionic topology using fins, which was identical to the leaf structure. The results showed that the employed asymmetrical fins boosted the melting rate and provided uniformity of temperature. Borhani et al. [28] conducted a comprehensive study to analyze the impact of helical fins, tilt angle, and fin thickness on PCM melting interval. The findings revealed that rising the spiral fin inclination decreases the full PCM melting time. However, increasing the thickness of the spiral fin adversely affects the system's performance. Zhang et al. [29] compared the melting properties of PCM in both the transversal and longitudinal axes for LHTES with several types of fins: annular, helical, longitudinal, and quadruple helical. It was found that various fin structures corresponded to various orientations. The vertical position of the annular fin and the helical fin provides better performance and a shorter melting time, unlike the longitudinal fin system and the quadruple fin system, which produce the best performance in the horizontal direction. Ghalambaz et al. [30] studied a three-tube LHTES system with twisted fins and compared it with LHS cases with and without longitudinal fins. The PCM occupied the annular region of the heat exchanger, and the water circulated in the opposite direction. The results revealed that using four twisted fins decreased melting time by 18% and 25%, respectively, compared to a unit with the same number of longitudinal fins and another one without fins. Yao and Huang [31] conducted a computational investigation on the solidification efficacy of paraffin in a triple tube using longitudinal triangular fins with varied distributions. The solidification duration was lowered by 30.98% when the triangular longitudinal fins were used

instead of traditional rectangular ones. Additionally, connecting position of all the fins on the external surface decreases the discharge duration by 13.61% compared with the fins connected to the inner tube. Abdulateef et al. [32] examined the impact of two types of fins: longitudinal and triangular inside a horizontal triplex tube. They discovered that the triangular fins accelerate the PCM melting 15% faster than the longitudinal fins.

Several studies [33, 34] have shown that adding fin arrays in a radial pattern (annular) along the circumference of the heat exchanger tube is a proven efficient way to improve thermal transmission in LHTES unit. Hassan et al. [35] performed an experimental examination of the fin shape influence on the PCM discharging process inside a TES system. Three fin designs were tested (annular, longitudinal and without fin). The results showed that utilizing annular fins enhances thermal performance when compared to other system designs. Furthermore, the findings show that using ring-shaped fins reduces melting time by more than 69%. It is also found that annular fins increase storage capacity by 52% compared with longitudinal fins. An experimental and numerical examination was performed by Kalabala et al. [36] on an annular fin unit. It was found that the melting time in a double LHTES tube with five annular fins of horizontal inclination is 85.63% greater compared with the vertical inclination. Yang et al. [37] evaluated the influence of the effect of fin arrangement and spacing in a TES unit. The results demonstrated that when non-uniformly distributed annular fins were used instead of evenly distributed ones, melting time and the average PCM temperature were reduced by 62.8% and 34.4%, respectively. Whereas, moving the fins down can lead to a uniform melting process. Furthermore, Elmaazouzi et al. [38] focused on a similar problem concerning the annular fin in TES system. They tested several fins geometrical configurations including length, thickness, number, and step. The outcomes revealed that the optimum addition of fins decreased both melting and solidification duration by 65.04% and 58.36%, respectively. Tiari et al. [39] conducted a computational study on the effect of annular fins with different lengths on PCM melting and solidification phases. They tested different fins' lengths and thicknesses by maintaining a constant volume occupied by the fins. They found that using 20 multi-length fins while keeping the longer ones at the bottom half part of the tube minimizes charging period by 73.7%. While, 20 fins of similar length answer the optimal design for the solidification process, which means about 79.2% reduction of time.

While extended surfaces provide a valuable advantage in enhancing heat transfer rates, they also cause a lot of disadvantages such as increasing weight, size, and cost. The challenge is therefore to improve heat transfer rate without significantly worsening the mentioned drawbacks. Addressing this challenge requires strategic thinking to develop innovative and effective solutions that lead to a careful balance between heat transfer performance, economics, and design considerations.

Previous studies [34, 40, 41] mainly focused on studying the impact of rectangular fin parameters such as length, thickness, spacing, inclination angles and number, in order to increase heat transfer within the PCM medium. In fact, the fins

not only improve heat transfer but also reduce the heat storage capacity of the TES unit, because some quantity of the PCM designated for storing thermal energy is replaced with fins. However, this problem has generally not been taken into account in investigations. Thus, in the current research, we try to study how to minimize the fins' impact on the heat storage capacity without compromising the heat transfer activity.

In this paper, a two-dimensional numerical simulation was carried out to explore the melting process of a vertically oriented LHTES heat exchanger with two types of fin shapes (rectangular and triangular) that occupied the same volume ratio of the PCM region. Firstly, the triangular and rectangular fin shapes are analyzed to examine their influence on the thermal efficiency of LHS. Afterwards, the effect of triangular fin spacing and height on the PCM melting process is investigated. Finally, we discuss the influence of the HTF inlet temperature on the PCM melting rate.

2. Numerical simulation

2.1. Physical design and computational domain

Fig. 1a and 1b show the 3D model of the annular finned tube heat exchanger unit and the cross-section along the heat transfer fluid (HTF) direction, respectively. The setup comprises two coaxial tubes with a length of $L = 400$ mm. The inner tube is composed of stainless steel, with a diameter of $D_c = 15$ mm and a thickness

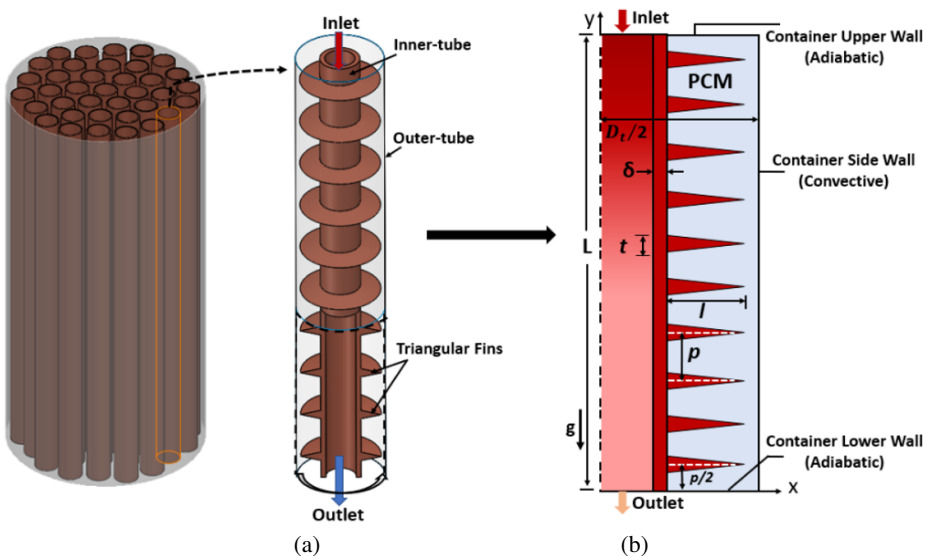


Fig. 1. Coaxial system featuring annular fins: (a) 3-D representation of triangular fin; (b) 2-D axisymmetric representation of triangular fin

of $\delta = 2.5$ mm. The outer tube, made of Perspex, has a diameter of $D_t = 44$ mm. Aluminum fins of a ring shape are connected to the exterior of the central tube. The variables l , t , and p represent the length, thickness, and spacing between the fins, respectively. Water maintained at a constant temperature serves as the HTF, flowing through the inner tube at a steady velocity of 0.01 m/s from top to bottom. For this investigation, Paraffin RT35 was chosen as the PCM, with a melting point of 308 K. The properties of the PCM, water, and aluminum are detailed in Table 1.

Table 1. Thermo-physical properties of PCM; aluminum and HTF [43]

Properties	PCM (RT35)	Fin (Aluminum)	HTF ($T = 325$ K)
Melting temperature, T_m (K)	308.15	–	–
Latent heat L ($\text{kJ}\cdot\text{kg}^{-1}$)	157	–	–
Density, ρ ($\text{kg}\cdot\text{m}^{-3}$)	880(s)/760(l)	2719	998.2
Specific heat capacity, cp ($\text{J}\cdot\text{kg}^{-1}\cdot\text{K}^{-1}$)	2400(s)/1800(l)	871	4182
Thermal conductivity, λ ($\text{W}\cdot\text{m}^{-1}\cdot\text{K}^{-1}$)	0.2	202.4	0.6
Dynamic viscosity, μ ($\text{kg}\cdot\text{m}^{-1}\cdot\text{s}^{-1}$)	0.0029	–	0.001003
Thermal expansion coefficient, β (K^{-1})	0.001	–	–

Five fin structures with the same volume ratio were numerically examined and details of their dimensions are given in Table 2. The case 1 has ten rectangular fins, which are transformed into ten triangular fins in case 2. Case 3 has five rectangular fins equivalent to ten triangular ones in case 4. The same arrangement is repeated in case 5 and case 6, where the number of ten rectangular fins doubles to twenty triangular ones. It should be noted that the length, thickness, and number of fins change in each case while maintaining the same size ratio of the fin, as shown in Fig. 2 and Fig. 3. Owing to the rotational symmetry, the physical setup is reduced to a 2D axisymmetric domain, considering the impact of gravity and natural convection.

Table 2. Fins dimensions of the studied cases including length, thickness, and numbers

	Fin volume ratio, V_f	Fin length, l (mm)	Thickness, t (mm)	Fin number, N
Case 1 (rectangular fin)	2%	5	2	10
Case 2 (triangular fins)		10	2	10
Case 3 (rectangular fin)		10	2	5
Case 4 (triangular fins)		10	2	10
Case 5 (rectangular fin)		10	1	10
Case 6 (triangular fins)		10	1	20

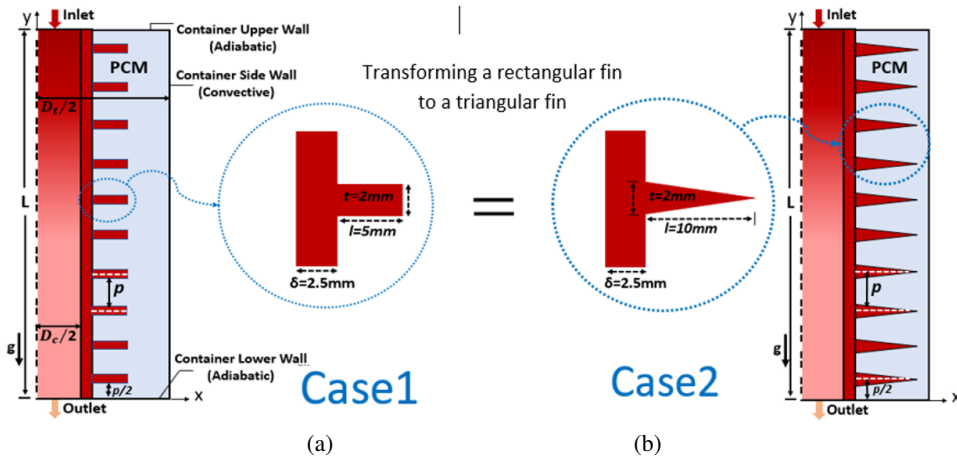


Fig. 2. Schematic of the TES unit with annular fins: Case 1 rectangular fin; Case 2 triangular fin

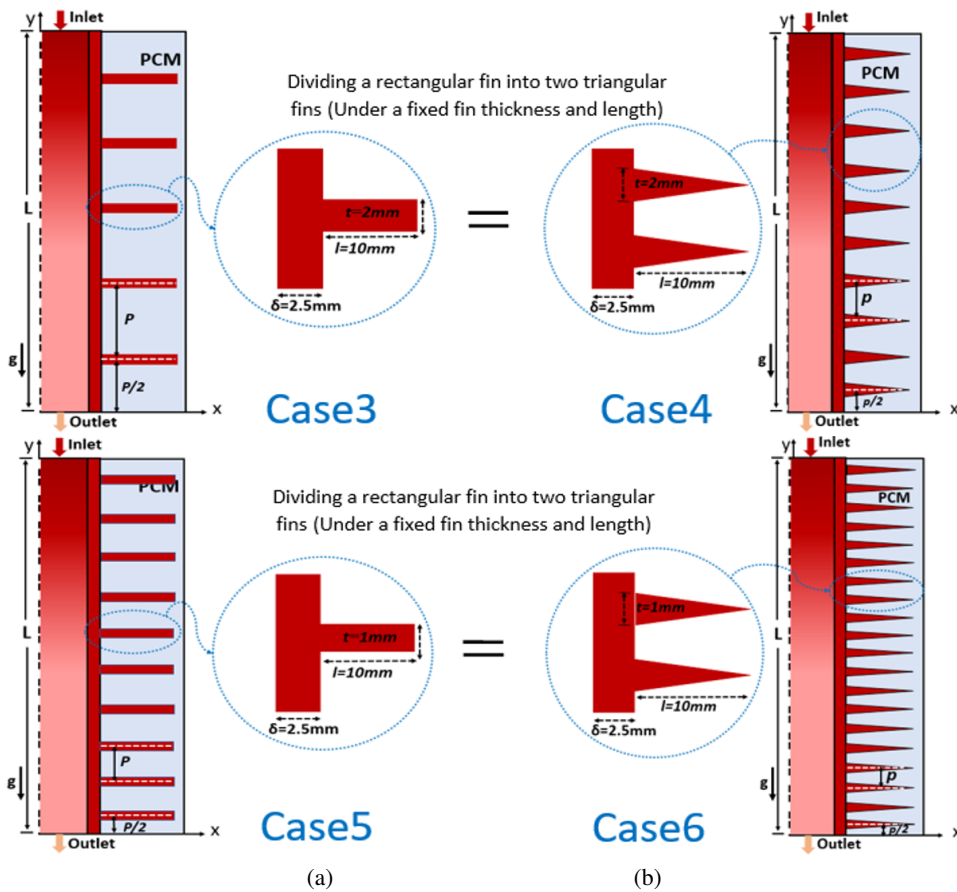


Fig. 3. Schematic of the TES unit with annular fins: (a) rectangular fins; (b) triangular fins

2.2. Governing equations

These assumptions were considered in the current numerical model:

- The model is bi-dimensional (2D) and axisymmetric.
- The HTF flow is laminar, Newtonian, and incompressible.
- Except for the PCM density and the specific heat capacity, all the thermo-physical properties of the PCM are considered constant.
- The thermal expansion coefficient related to the phase change has been considered.

The transient phase change heat transfer with local natural convection is governed by the following equations:

Continuity equation

$$\nabla \cdot \vec{u} = 0. \quad (1)$$

Momentum equation

$$\rho \frac{\partial(\vec{u})}{\partial t} + \rho (\vec{u} \cdot \nabla) \vec{u} = -\nabla p + \mu \nabla^2 \vec{u} + S_b + S. \quad (2)$$

Energy equation

$$\rho C_p \frac{\partial T}{\partial t} + \rho C_p \vec{u} \cdot \nabla T = \nabla \cdot (\lambda \nabla T) - \rho L \frac{\partial \gamma}{\partial t}. \quad (3)$$

The phase transition process is simulated employing the enthalpy-porosity method [42], where the solid-liquid interface is conceptualized as a porous medium. This method allows for a continuous change in the liquid fraction across the 'mushy zone', with porosity values ranging from 0 in the solid phase to 1 in the liquid phase. The momentum source term is presented as:

$$s = C \frac{(1 - \gamma)^2}{\gamma^3 + \delta} \vec{u}. \quad (4)$$

The parameter C denotes a constant that characterizes the shape of the melting interface within the mushy region. It is recommended to constrain its value within the range of (10^4 to 10^7). Additionally, to prevent the occurrence of dividing by zero, a small value of $\delta = 0.001$ is employed. Here, u_i represents the liquid phase's flow velocity in the PCM.

As the PCM temperature changes between solidus and liquidus phases, γ refers to the liquid fraction varying between 0 and 1 and is defined as:

$$\gamma = \begin{cases} 0, & T < T_s, \\ \frac{T - T_s}{T_l - T_s}, & T_s < T < T_l, \\ 1, & T > T_l. \end{cases} \quad (5)$$

Boussinesq approximation was adopted to calculate the change in PCM density as a function of temperature in the liquid density given by:

$$S_b = \rho_{\text{ref}} g \beta (T - T_m), \quad (6)$$

where ρ_{ref} is the reference density of the liquid PCM at melting temperature T_m , β thermal expansion coefficient.

For the HTF, the fluid flow and convective heat transfer are governed by the following equations:

$$\nabla \cdot \vec{u} = 0, \quad (7)$$

$$\rho_{\text{HTF}} \frac{\partial \vec{u}}{\partial t} + \rho_{\text{HTF}} (\vec{u} \cdot \nabla) \vec{u} = -\nabla p + \mu_{\text{HTF}} \nabla^2 \vec{u}, \quad (8)$$

$$\rho_{\text{HTF}} C_{p\text{HTF}} \frac{\partial T}{\partial t} + \rho_{\text{HTF}} C_{p\text{HTF}} \vec{u} \cdot \nabla T = \nabla \cdot (\lambda_{\text{HTF}} \nabla T). \quad (9)$$

Conjugate heat transfer is considered at the interface between HTF and tube wall:

$$T_{\text{HTF}} = T_{\text{tube}}, \quad \lambda_{\text{HTF}} \frac{\partial T_{\text{HTF}}}{\partial n} = \lambda_{\text{tube}} \frac{\partial T_{\text{tube}}}{\partial n}. \quad (10)$$

Here, ρ_{HTF} , $c_{p\text{HTF}}$ and λ_{HTF} are separately the density, specific heat and thermal conductivity; T is temperature; t denotes time; subscripts HTF and tube stand for HTF and heat transfer tube, in respective.

2.3. Initial and boundary conditions

The initial inlet HTF velocity (u) and the temperature (T_0) of the whole studied domain are given by the equation (10).

$$t = 0, \quad T = T_0, \quad u = 0, \quad v = 0. \quad (11)$$

The initial HTF temperature and velocity at the tube inlet were defined as follows:

$$T_{\text{in}} = 325 \text{ K}, \quad u = 0.01 \text{ ms}^{-1}, \quad v = 0. \quad (12)$$

The conditions at the coordinate $x = 0$ mm

$$x = 0, \quad v = 0, \quad \frac{\partial u}{\partial y} = 0, \quad \frac{\partial T}{\partial y} = 0. \quad (13)$$

The upper and lower walls are thermally insulated:

$$\frac{\partial T}{\partial y} = 0. \quad (14)$$

The temperature difference between the Perspex wall and the surrounding temperature still results in heat loss, even though the thermal conductivity of

the Perspex walls is low. The natural convection heat transfer coefficient can be computed by:

$$h = \frac{\text{Nu}\lambda}{D}, \quad (15)$$

where λ and Nu represent the thermal conductivity of air and the Nusselt number, respectively, and D represents the length of the LHTES.

The boundary condition of the Perspex wall is:

$$-\lambda \frac{\partial T}{\partial n} = h(T - T_0), \quad (16)$$

where T_0 is the ambient temperature.

3. Numerical procedure and validation

3.1. Numerical procedure

The phenomena under investigation are addressed using Ansys Fluent, where the equations controlling these phenomena are solved. For the coupling of pressure and velocity, the SIMPLE algorithm is employed [44], while the convection terms are discretized using the QUICK scheme, and the PRESTO scheme is applied to get the pressure correction. Buoyancy forces resulting from temperature gradients during phase transition are accounted for using the Boussinesq approximation. Finally, the convergence criteria for the governing equations are set at 10^{-8} for energy and 10^{-5} for momentum and continuity.

3.2. Grid and time step independence study

In general, the numerical simulation of any physical phenomenon is influenced by the grid's structures and the time step size.

Fig. 4a presents the variation of the melting fraction versus different cell numbers considered to examine the independence of the grid. Three various mesh numbers (4900, 19600 and 39200 grids) were investigated. It can be observed that the differences in results between the cases of 19600 and 39200 grids are small and negligible; thus, the cell number of 19600 was adopted the whole numerical calculations.

The findings of the transient simulation regarding the solid-liquid phase transition process exhibit a high degree of sensitivity to the selected time step size. To ensure the robustness of the results independent of the time step size, we compared three different time step sizes: 0.1 s, 0.5 s, and 1 s. As illustrated in Fig. 4b, we found that the relative deflection is very small. Consequently, for all subsequent simulations, we adopted a cell count of 19,600 grids and a time step size of 0.1s. This selection not only conserves computational resources but also validates the accuracy of the results.

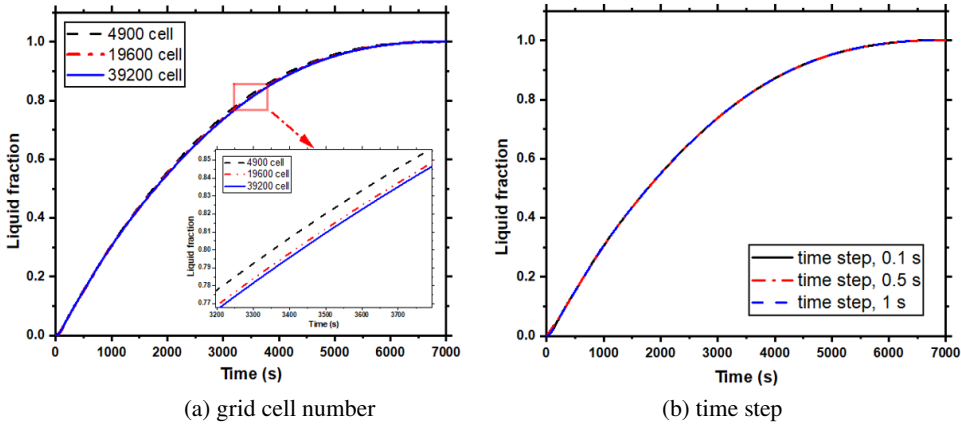


Fig. 4. Time step and mesh size independency tests

3.3. Validation

We validated the present model by comparing it with the experimental and numerical findings of Martin et al. [43].

This validation is performed in a 2-D simulation of a vertical LHTES unit, considering the same initial and boundary conditions, including material properties, operation conditions and geometry parameters as Martin et al. [43]. The temperature evolution was recorded at two fixed points (section D), as shown in Fig. 5a, during charging with top HTF injection. According to Fig. 5b, the good agreement achieved by our model confirms its precision.

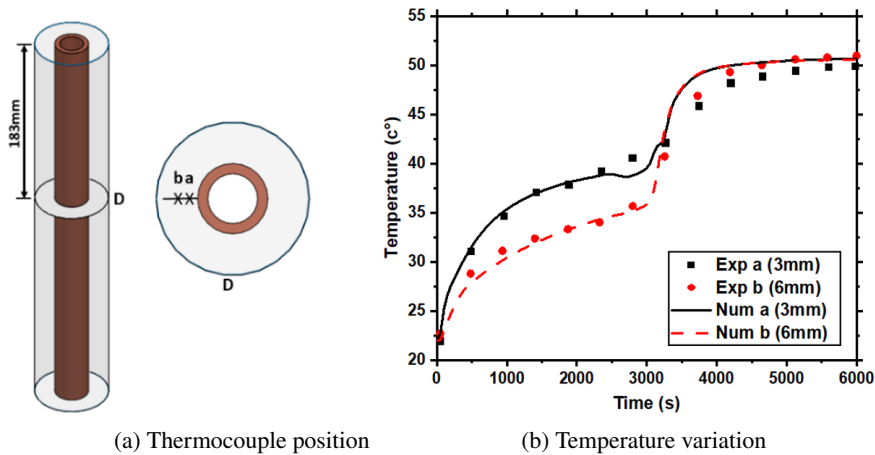


Fig. 5. Comparison of the experimental results and numerical solution

4. Results and discussion

4.1. Effect of fin shape design on melting process

As depicted in Fig. 2, case 1 involves 10 rectangular fins with a dimension of 2×5 mm (base thickness \times length). In case 2, rectangular fins are transformed into triangular ones, increasing their length to 10 mm while preserving the total area occupied by the fins as a constant (2% from the whole PCM region) (see Table 2).

The comparative analysis in Fig. 6 shows that the PCM melting process is faster in case 2 compared to case 1. This is mainly because the rectangular fins are unable to easily access the solid PCM located between the straight fins and the outer wall. Consequently, the melting process takes significantly longer due to the strong PCM thermal resistance. By changing the shape of the fins to triangular (case 2) with the same volume ratio, their surface area and length increase, where the first parameter accelerates the heat transfer rate, while the second allows heat to be transferred deeper into the PCM. Thus, it reduces the PCM melting time by 12.64% compared to rectangular fins. It should therefore be noted that for the same size of the fins, the triangular shape is more efficient than the rectangular one for the same base thickness because it allows primarily an enlargement of the heat transfer surface area, as shown in Fig. 3, which speeds up the PCM melting process, and additionally gives the fin a longer shape that enables it to reach deeper regions inside the PCM.

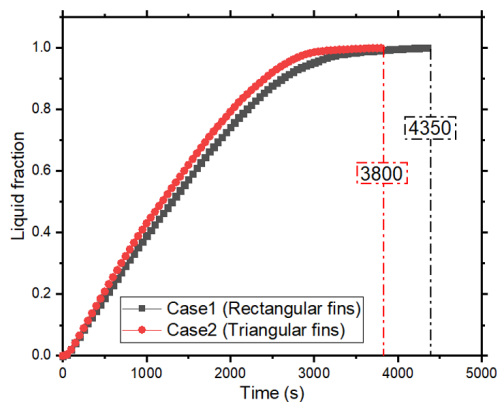


Fig. 6. Variation of liquid fraction versus time

4.2. Effect of fin design parameters

The application of rectangular fins represents a prominent strategy to enhance the thermal efficiency of LHTES unit used in thermal engineering. However, based on the outcomes of the previous section (4.1) and the above reference [38], the significance of fin length becomes evident. For the best understanding of other

parameters, we extended our investigation to the thickness of fin base attached to the inner tube. By fixing the fin length to 10 mm, and assuming its base thickness of 1 to 2 mm, we obtain four different TES units, where the number of triangular fins is doubled compared to the rectangular ones for each thickness, as mentioned in Table 2.

The melting fraction (M_f) serves as a very important parameter for effectively illustrating the impact of various fin designs on the PCM melting operation. Fig. 7 represents the contours of liquid fraction and streamlines throughout the melting process for the cases under examination.

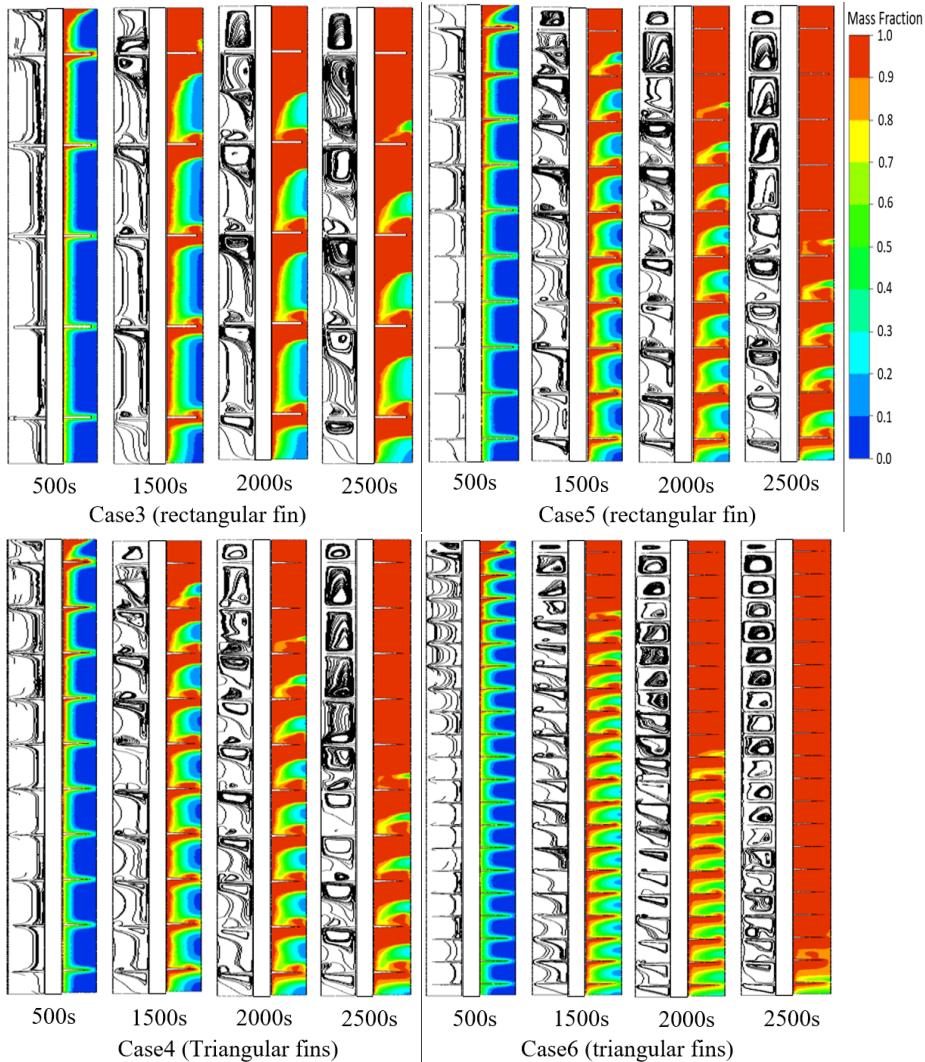


Fig. 7. Velocity (left) and liquid fraction (right) contours using triangular or rectangular fins at $h = 10$ mm

At the beginning of this process, almost all the cases show the same behavior: the liquid portion of the PCM expands with the heat transmission wall and shape of the fin due to direct contact between them. But as the time goes on, the PCM liquid phase layer becomes larger and forms small eddies between the fins, as appears in Fig. 7 at 1500 s. With the passage of time, particularly at $t = 2000$ s and $t = 2500$ s, the small eddies progressively recombine to form a large vortex between the fins and the inner surface of the Perspex, due to the natural convection.

Essentially, the transfer of thermal energy occurs because of the density gradient, meaning that the fluid with higher density moves towards the bottom while the fluid with lower density moves towards the top. According to the melting contours, the LHTES cavity with a triangular fin design (case 6) shows a larger area of melted PCM compared to the rest of configurations. This is attributed to the large number of fins in the container, which consequently extends the heat exchange area. Also, it is worth mentioning that the addition of triangular fins not only subdivides the PCM into smaller regions but also enhances both conduction and convection heat transmission rates.

In addition, Fig. 8 shows the complete melting time of PCM for all cases. The results showed that a TES unit without fins needed 6600 seconds to complete a full charging cycle. Whereas it took 4350 s, 3800 s, 3750 s, and 3250 s for Case 3, Case 4, Case 5 and Case 6, respectively. These configurations reduced the total melting time by 34.09%, 42.42%, 43.18%, and 50.75%, respectively, compared to the case without fins.

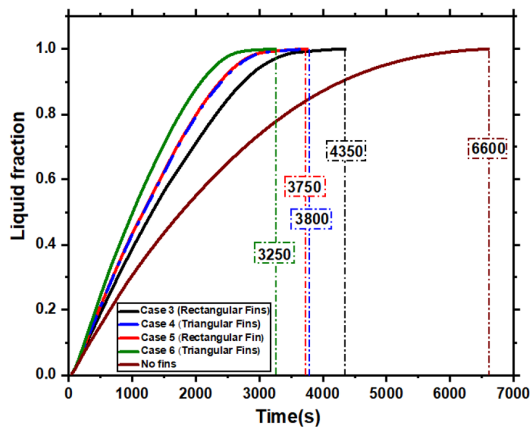


Fig. 8. The average melting fraction using triangular or rectangular fins at $l = 10$ mm

Comparing the results, we find that using 20 triangular fins instead of 10 rectangular ones of the same length (10 mm), thickness (1 mm), and occupied area (2%) can lower the entire required period for PCM melting by 15.38%. Hence, opting for triangular fins over conventional rectangular ones represents an efficient approach that maximizes the heat transmission region between the fins and

the PCM. Therefore, the subsequent sections focus on analyzing various physical parameters of the triangular fins.

4.3. Effect of fin spacing and length

The influence of the space between fins and its length on the PCM melting phase is evaluated in this part. The most relevant studies on this subject are those of Pu et al. [45]. Enhancing the heat transfer region promotes the dynamic heat transmission from the fin to the PCM. However, a higher number of fins also results in increased thermal conduction resistance in the fin area, consequently raising the cost and weight of the TES unit without significant improvement in heat transfer performance. To ensure a reliable comparison, we considered that the whole area equipped by fins represents 2% of the entire volume of PCM, with a constant fin thickness of 1 mm. Therefore, six units with fin lengths of 0 mm, 5 mm, 5.7143 mm, 6.6667 mm, 8 mm, and 10 mm are proposed. As the fin length increases from 5 to 10, the number of fins decreases from 40 to 20, while the fin spacing increases from 10 to 20 mm. The structural parameters of different fin lengths are recapitulated in Table 3. Fig. 9 presents the temperature and liquid fraction distributions for various fin lengths at different stages.

Table 3. Finned TES unit parameters for a fin volume ratio (2%) and fin thickness (1 mm)

Fin volume ratio, V_f	Thickness, t (mm)	Fin length, l (mm)	Fin number, N	Fin spacing, p (mm)
2%	1	5	40	10
		5.7143	35	11.4286
		6.6667	30	13.3333
		8	25	16
		10	20	20

In the initial phase ($t = 500$ s), the PCM in all the studied cases begins to melt, resulting in the formation of a thin layer along the adjacent heated wall and fin surfaces primarily due to predominant heat conduction. Besides, as shown in Fig. 9, a difference in thickness of the molten PCM is evident between the upper and lower sections of the tube. In fact, the reason behind it is the significant gradient in HTF temperature between the top and the bottom due to the heat transmission along the flow direction. Over the time, the solid to the liquid PCM transition decelerates gradually in the presence of small fins. This is attributed to the fins length which is too small to cover most of the PCM's region, leading to a significant decrease in the thermal resistance between the hot water and the PCM. As the fin length increases, despite the fact that the spacing between the fins expands, the melting rate of the PCM increases. This occurs due to the high thermal conductivity of the fin material, which enables even distribution of heat across most of the phase change area.

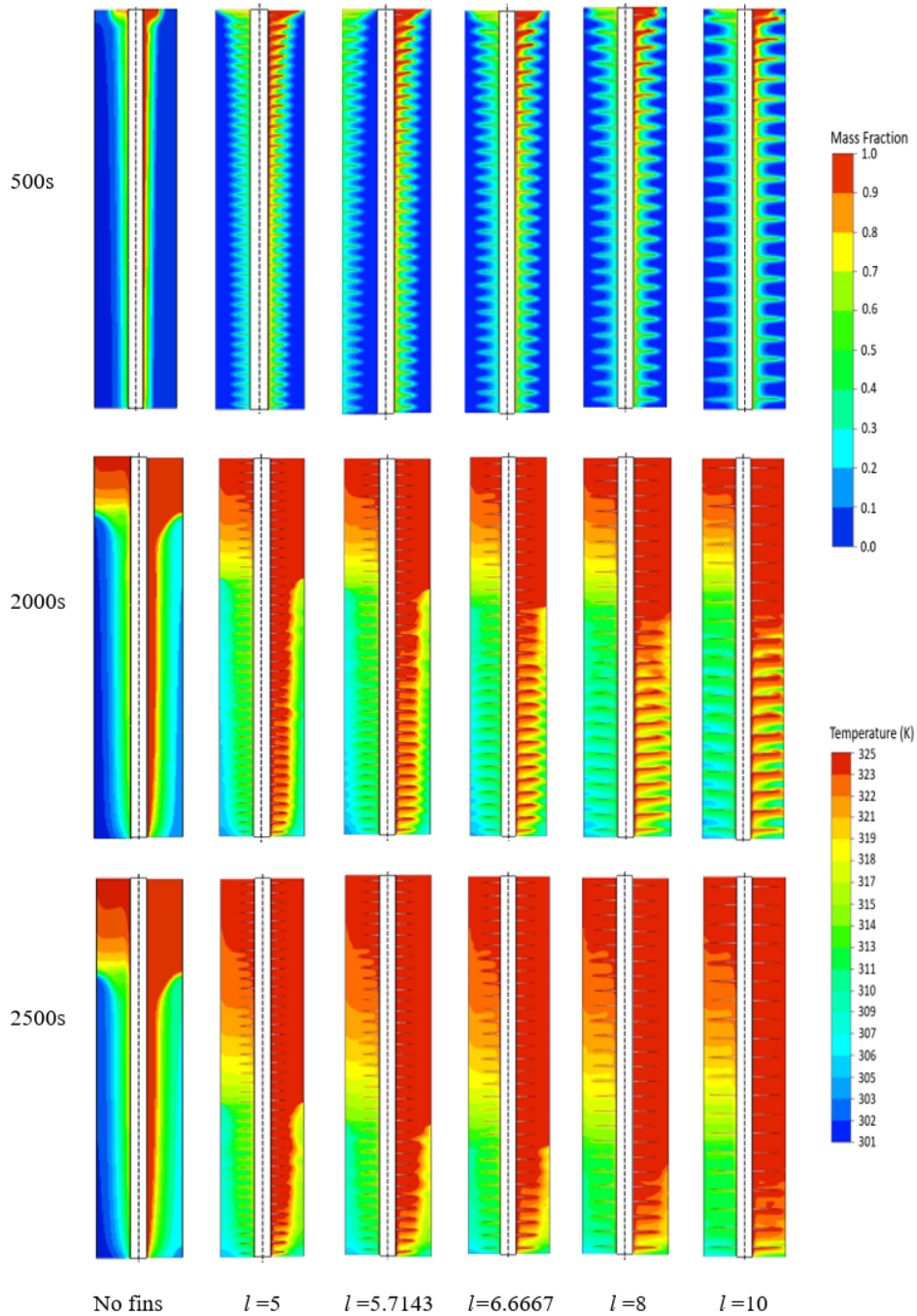


Fig. 9. Temperature (left) and liquid fraction (right) contours for LHTES units with different fin spacing and length

The time required for the full melting of PCM varies with the fin spacing and length, as shown in Fig. 10 and Fig. 11. For the cases with fins' length of 5, 5.7143, 6.6667, 8, and 10 mm, the full PCM melting time takes 3950 s, 3750 s, 3600 s, 3400 s and 3250 s, respectively, which reduces melting time by 40.15%, 43.18%, 45.45%, 48.48% and 50.75%, respectively, comparing to the case without fins. Therefore, it is obvious that the longer the fins, the shorter the full melting time.

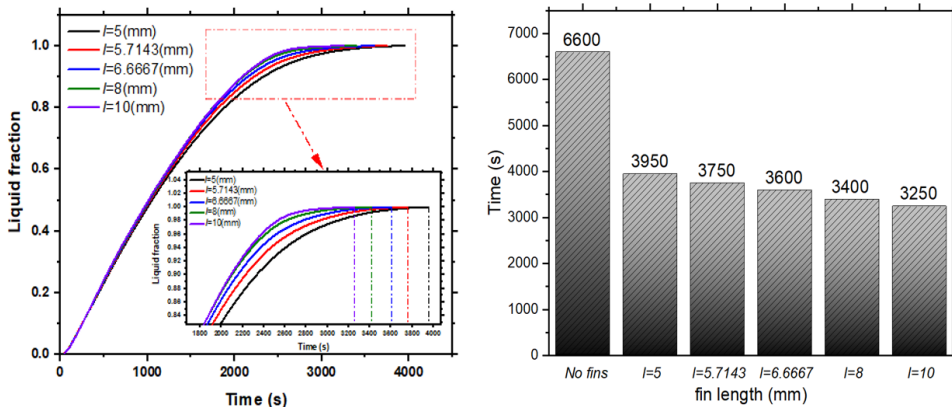


Fig. 10. Effect of fin spacing and length on liquid fraction

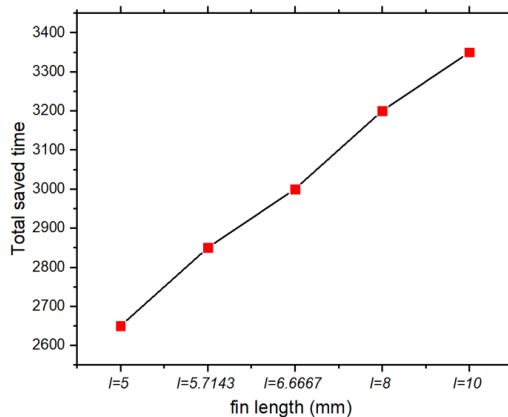


Fig. 11. Total saved time when compared to base case (without fins)

4.4. Temperature history curve

The PCM axial temperature curve along the HTF flow direction was investigated. The entire system was divided into 5 axial sections with similar dimensions (80 mm each). Measurement lines (A to D) are placed between fins at the locations shown in Fig. 12b. In fact, the LHTES unit without fins takes more time for the

full PCM's melting, especially at the bottom, because the HTF loses a lot of its thermal energy in the upper regions. The use of fins can overcome this problem. It is apparent that the PCM in the line D region requires more time to melt. Melting time is about 4500 s while, for the same position in the unit with fins, this time is reduced by 2500 s, as shown in Fig. 12a. This due to the large temperature gradient within the PCM, which is reduced by using the fins.

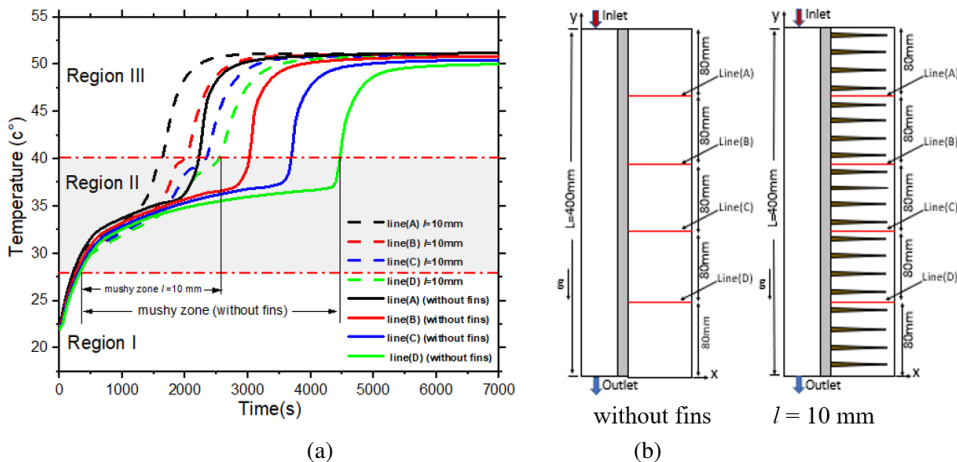


Fig. 12. Temperature distributions of different selected lines: (a) temperature measurement locations; (b) temperature change at the selected locations

Regarding the full PCM melting time, the whole PCM temperature curve can be divided into three regions: the cold sensible region (Region I), the latent region (Region II), and the hot sensible region (Region III). In the first region, the temperature gradient between the hot water and PCM rises significantly, which causes the temperature to increase slightly faster in the early stages until it approaches the PCM melting point. At the same time, we observe a negligible difference in temperature between different locations. The next zone represents the area most significant for the LHTES system. The PCM temperature with fins rises rapidly at the phase change point within the range of 1550–3100 s and then slowly decreases to the final stage of the melting process. Likewise, the duration of the mushy zone shortens with increasing fin length, which shows that increasing the length of the fins along the radial direction greatly increases the heat transmission rate and provides a perfect temperature uniformity inside the TES system. When the fin length is increased from $h = 0$ mm to $h = 10$ mm, the full PCM melting time at line (D) is reduced by approximately 6800 and 3500 s, respectively. Thus, increasing the fin length improves the full heat transmission mechanisms within the LHTES system.

4.5. Effect of HTF temperature

Fig. 13 shows the liquid fraction curves and the total PCM melting durations at various inlet HTF temperatures. Specifically, Fig. 13a demonstrates that higher inlet water temperatures create a more pronounced temperature gradient between the PCM and water, which leads to reducing the melting duration. Furthermore, as seen in Fig. 13b, the time difference decreases as HTF temperature increases. Thus, the timeframe for achieving complete melting in the triangular fin design unit (case 6) displays variability across different water temperatures. For example, with an increase in HTF temperature from 325.15 K to 345.15 K, the melting interval sharply decreases from 3250 s to 1750 s, resulting in a reduction by 46.16%. While the melting time decreases by 17.14% when the HTF temperature increases to 355.15 K. The reason behind it is the large amount of heat transmitted to the PCM. This means that beyond a certain temperature difference, the melting time stabilized.

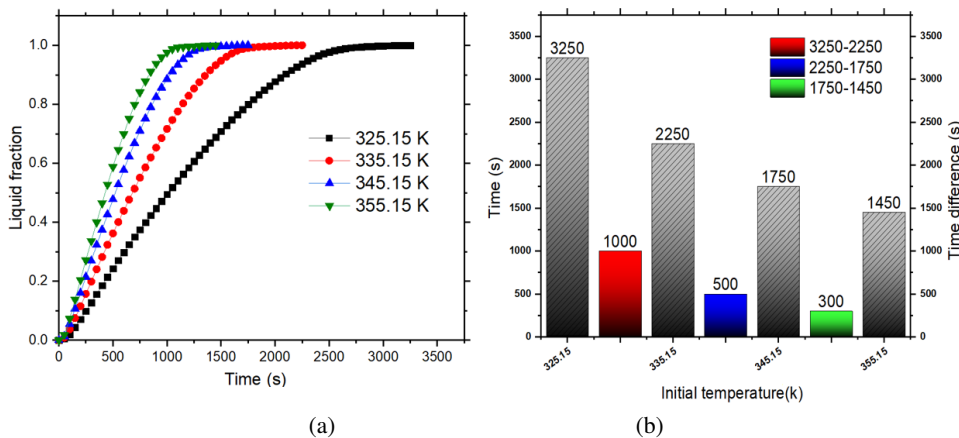


Fig. 13. TEeffect of temperature difference HTF and PCM on melting behavior: (a) melting fraction; (b) setting time required

5. Conclusions

Thermal efficiency improvement of a LHTES container with ring-shaped fins was numerically examined. In fact, application of the fins is the most suitable and powerful means for improving thermal performance in an LHTES systems. However, the effectiveness of the fins depends on various design parameters, such as their shape, thickness, spacing, and length. In this study, we examined two types of fin shape, rectangular and triangular that occupied the same surface area to the PCM. After finding the best case, the combined influence of fins spacing and length on the PCM melting behavior was evaluated. Besides, the influence of various HTF

inlet temperatures was also discussed. The outcomes of the present investigation are summarized as follows:

- The current study showed that replacing rectangular fins with triangular ones of the same length, base thickness, and occupied area allows for doubling their number. Thus, it increases the heat transfer surface area without compromising the heat storage capacity of the TES unit.
- Using an equal number of rectangular and triangular fins occupying identical surface area makes it possible to increase both the heat transfer area and the length of triangular fins compared to rectangular fins which reduces the PCM melting time by 12.65%.
- The best results achieved by application of the triangular shape fins compared to rectangular ones have shown that small changes in design lead to a great improvement in performance.
- Whatever the number of fins, the longest ones have the best effect on PCM melting rate, which increases due to the improving heat transfer away from the hot inner tube.
- For the same whole surface area of fins; the length has a more significant effect than the spacing, which means that a LHTES unit with 20 tall fins provides better thermal performance than another with 40 small fins.
- The performance of LHTES heat storage can be effectively enhanced by rising the inlet temperature of HTF. Thus, it is suitable to select a HTF temperature 20 K greater than the PCM melting point.

Acknowledgements

We gladly acknowledge the financial support from the General Directorate for Scientific Research and Technological Development (DG-RSDT) and Algerian Ministry of High Education and Scientific Research.

Project PRFU Number: A11N01UN380120220001.

References

- [1] V. Bhatale, N. Vivekananda, and C. Shriramshastri. Experimental assessment of a PCM to air heat exchanger storage system for building ventilation applications. *International Journal of Current Engineering and Technology*, 6(spec.iss.5):413–418, 2016. doi: [10.14741/ijcet/22774106/spl.5.6.2016.77](https://doi.org/10.14741/ijcet/22774106/spl.5.6.2016.77).
- [2] M. Ryms and E. Klugmann-Radziemska. Possibilities and benefits of a new method of modifying conventional building materials with phase-change materials (PCMs). *Construction and Building Materials*, 211:1013–1024, 2019. doi: [10.1016/j.conbuildmat.2019.03.277](https://doi.org/10.1016/j.conbuildmat.2019.03.277).
- [3] F. Souayfane, F. Fardoun, and P.H. Biwole. Phase change materials (PCM) for cooling applications in buildings: A review. *Energy and Buildings*, 129:396–431, 2016. doi: [10.1016/j.enbuild.2016.04.006](https://doi.org/10.1016/j.enbuild.2016.04.006).
- [4] N.I. Ibrahim, F.A. Al-Sulaiman, S. Rahman, B.S. Yilbas, and A.Z. Sahin. Heat transfer enhancement of phase change materials for thermal energy storage applications: A critical review. *Renewable and Sustainable Energy Reviews*, 74:26–50, 2017. doi: [10.1016/j.rser.2017.01.169](https://doi.org/10.1016/j.rser.2017.01.169).

- [5] A. Sciacovelli, F. Gagliardi, and V. Verda. Maximization of performance of a PCM latent heat storage system with innovative fins. *Applied Energy*, 137:707–715, 2015. doi: [10.1016/j.apenergy.2014.07.015](https://doi.org/10.1016/j.apenergy.2014.07.015).
- [6] C. Zhang, J. Li, and Y. Chen. Improving the energy discharging performance of a latent heat storage (LHS) unit using fractal-tree-shaped fins. *Applied Energy*, 259:114102, 2020. doi: [10.1016/j.apenergy.2019.114102](https://doi.org/10.1016/j.apenergy.2019.114102).
- [7] X. Yang, Z. Lu, Q. Bai, Q. Zhang, L. Jin, and J. Yan. Thermal performance of a shell-and-tube latent heat thermal energy storage unit: Role of annular fins. *Applied Energy*, 202:558–570, 2017. doi: [10.1016/j.apenergy.2017.05.007](https://doi.org/10.1016/j.apenergy.2017.05.007).
- [8] C. Ji, Z. Qin, Z. Low, S. Dubey, F. H. Choo, and F. Duan. Non-uniform heat transfer suppression to enhance PCM melting by angled fins. *Applied Thermal Engineering*, 129:269–279, 2018. doi: [10.1016/j.applthermaleng.2017.10.030](https://doi.org/10.1016/j.applthermaleng.2017.10.030).
- [9] J. Guo, Z. Liu, Z. Du, J. Yu, X. Yang, and J. Yan. Effect of fin-metal foam structure on thermal energy storage: An experimental study. *Renewable Energy*, 172: 57–70, 2021. doi: [10.1016/j.renene.2021.03.018](https://doi.org/10.1016/j.renene.2021.03.018).
- [10] N. Zhang and Y. Yuan. Synthesis and thermal properties of nanoencapsulation of paraffin as phase change material for latent heat thermal energy storage. *Energy and Built Environment*, 1(4):410–416, 2020. doi: [10.1016/j.enbenv.2020.04.003](https://doi.org/10.1016/j.enbenv.2020.04.003).
- [11] N.S. Bondareva, B. Buonomo, O. Manca, and M.A. Sheremet. Heat transfer inside cooling system based on phase change material with alumina nanoparticles. *Applied Thermal Engineering*, 144:972–981, 2018. doi: [10.1016/j.applthermaleng.2018.09.002](https://doi.org/10.1016/j.applthermaleng.2018.09.002).
- [12] M. Ghalambaz, H. Jin, A. Bagheri, O. Younis, and D. Wen. Convective flow and heat transfer of nano-encapsulated phase change material (NEPCM) dispersions along a vertical surface. *Facta Universitatis, Series: Mechanical Engineering*, 20(3):519–538, 2022. doi: [10.22190/FUME220603034G](https://doi.org/10.22190/FUME220603034G).
- [13] I. Daou, L. El-Kaddadi, O. Zegaoui, M. Asbik, and N. Zari. Structural, morphological and thermal properties of novel hybrid-microencapsulated phase change materials based on Fe₂O₃, ZnO and TiO₂ nanoparticles for latent heat thermal energy storage applications. *Journal of Energy Storage*, 17:84–92, 2018. doi: [10.1016/j.est.2018.02.011](https://doi.org/10.1016/j.est.2018.02.011).
- [14] Z. Huang, X. Gao, T. Xu, Y. Fang, and Z. Zhang. Thermal property measurement and heat storage analysis of LiNO₃/KCl – expanded graphite composite phase change material. *Applied Energy*, 115:265–271, 2014. doi: [10.1016/j.apenergy.2013.11.019](https://doi.org/10.1016/j.apenergy.2013.11.019).
- [15] K. Merlin, J. Soto, D. Delaunay, and L. Traonvouez. Industrial waste heat recovery using an enhanced conductivity latent heat thermal energy storage. *Applied Energy*, 183:491–503, 2016. doi: [10.1016/j.apenergy.2016.09.007](https://doi.org/10.1016/j.apenergy.2016.09.007).
- [16] V. Joshi and M.K. Rathod. Experimental and numerical assessments of thermal transport in fins and metal foam infused latent heat thermal energy storage systems: A comparative evaluation. *Applied Thermal Engineering*, 178:115518, 2020. doi: [10.1016/j.applthermaleng.2020.115518](https://doi.org/10.1016/j.applthermaleng.2020.115518).
- [17] H. Masoumi, R. Haghghi Khoshkhou, and S.M. Mirfendereski. Experimental and numerical investigation of melting/solidification of nano-enhanced phase change materials in shell & tube thermal energy storage systems. *Journal of Energy Storage*, 47:103561, 2022. doi: [10.1016/j.est.2021.103561](https://doi.org/10.1016/j.est.2021.103561).
- [18] S.Z. Tang, H.Q. Tian, J.J. Zhou, and H. Li. Evaluation and optimization of melting performance in a horizontal thermal energy storage unit with non-uniform fins. *Journal of Energy Storage*, 33:102124, 2021. doi: [10.1016/j.est.2020.102124](https://doi.org/10.1016/j.est.2020.102124).
- [19] M. Kazemi, M.J. Hosseini, A.A. Ranjbar, and R. Bahrampoury. Improvement of longitudinal fins configuration in latent heat storage systems. *Renewable Energy*, 116(A):447–457, 2018. doi: [10.1016/j.renene.2017.10.006](https://doi.org/10.1016/j.renene.2017.10.006).

- [20] H.B. Mahood, M.S. Mahdi, A.A. Monjezi, A.A. Khadom, and A.N. Campbell. Numerical investigation on the effect of fin design on the melting of phase change material in a horizontal shell and tube thermal energy storage. *Journal of Energy Storage*, 29:101331, 2020. doi: [10.1016/j.est.2020.101331](https://doi.org/10.1016/j.est.2020.101331).
- [21] A.H.N. Al-Mudhafar, A.F. Nowakowski, and F.C.G.A. Nicolleau. Performance enhancement of PCM latent heat thermal energy storage system utilizing a modified webbed tube heat exchanger. *Energy Reports*, 6(suppl.5):76–85, 2020. doi: [10.1016/j.egy.2020.02.030](https://doi.org/10.1016/j.egy.2020.02.030).
- [22] T. Bouhal, S. ed-Dîn Fertahi, T. Kousksou, and A. Jamil. CFD thermal energy storage enhancement of PCM filling a cylindrical cavity equipped with submerged heating sources. *Journal of Energy Storage*, 18:360–370, 2018. doi: [10.1016/j.est.2018.05.015](https://doi.org/10.1016/j.est.2018.05.015).
- [23] J. Zheng, J. Wang, T. Chen, and Y. Yu. Solidification performance of heat exchanger with tree-shaped fins. *Renewable Energy*, 150:1098–1107, 2020. doi: [10.1016/j.renene.2019.10.091](https://doi.org/10.1016/j.renene.2019.10.091).
- [24] M. Zhao, Y. Tian, M. Hu, F. Zhang, and M. Yang. Topology optimization of fins for energy storage tank with phase change material. *Numerical Heat Transfer, Part A: Applications*, 77(3):284–301, 2020. doi: [10.1080/10407782.2019.1690338](https://doi.org/10.1080/10407782.2019.1690338).
- [25] A. Pizzolato, A. Sharma, K. Maute, A. Sciacovelli, and V. Verda. Topology optimization for heat transfer enhancement in Latent Heat Thermal Energy Storage. *International Journal of Heat and Mass Transfer*, 113:875–888, 2017. doi: [10.1016/j.ijheatmasstransfer.2017.05.098](https://doi.org/10.1016/j.ijheatmasstransfer.2017.05.098).
- [26] A. Pizzolato, A. Sharma, R. Ge, K. Maute, V. Verda, and A. Sciacovelli. Maximization of performance in multi-tube latent heat storage – Optimization of fins topology, effect of materials selection and flow arrangements. *Energy*, 203:114797, 2020. doi: [10.1016/j.energy.2019.02.155](https://doi.org/10.1016/j.energy.2019.02.155).
- [27] Y. Tian, et al. Bionic topology optimization of fins for rapid latent heat thermal energy storage. *Applied Thermal Engineering*, 194:117104, 2021. doi: [10.1016/j.applthermaleng.2021.117104](https://doi.org/10.1016/j.applthermaleng.2021.117104).
- [28] S.M. Borhani, M.J. Hosseini, A.A. Ranjbar, and R. Bahrapoury. Investigation of phase change in a spiral-fin heat exchanger. *Applied Mathematical Modelling*, 67:297–314, 2019. doi: [10.1016/j.apm.2018.10.029](https://doi.org/10.1016/j.apm.2018.10.029).
- [29] S. Zhang, L. Pu, L. Xu, R. Liu, and Y. Li. Melting performance analysis of phase change materials in different finned thermal energy storage. *Applied Thermal Engineering*, 176:115425, 2020. doi: [10.1016/j.applthermaleng.2020.115425](https://doi.org/10.1016/j.applthermaleng.2020.115425).
- [30] M. Ghalambaz, J.M. Mahdi, A. Shafaghat, A.H. Eisapour, O. Younis, P.T. Sardari, and W. Yaici. Effect of twisted fin array in a triple-tube latent heat storage system during the charging mode. *Sustainability*, 13(5):2685, 2021. doi: [10.3390/su13052685](https://doi.org/10.3390/su13052685).
- [31] S. Yao and X. Huang. Study on solidification performance of PCM by longitudinal triangular fins in a triplex-tube thermal energy storage system. *Energy*, 227:120527, 2021. doi: [10.1016/j.energy.2021.120527](https://doi.org/10.1016/j.energy.2021.120527).
- [32] A.M. Abdulateef, S. Mat, K. Sopian, J. Abdulateef, and A.A. Gitan. Experimental and computational study of melting phase-change material in a triplex tube heat exchanger with longitudinal/triangular fins. *Solar Energy*, 155:142–153, 2017. doi: [10.1016/j.solener.2017.06.024](https://doi.org/10.1016/j.solener.2017.06.024).
- [33] Y.K. Liu and Y.B. Tao. Experimental and numerical investigation of longitudinal and annular finned latent heat thermal energy storage unit. *Solar Energy*, 243:410–420, 2022. doi: [10.1016/j.solener.2022.08.023](https://doi.org/10.1016/j.solener.2022.08.023).
- [34] Y. Zhang, G. Yuan, Y. Wang, P. Gao, C. Fan, and Z. Wang. Solidification of an annular finned tube ice storage unit. *Applied Thermal Engineering*, 212:118567, 2022. doi: [10.1016/j.applthermaleng.2022.118567](https://doi.org/10.1016/j.applthermaleng.2022.118567).
- [35] A.K. Hassan, J. Abdulateef, M.S. Mahdi, and A.F. Hasan. Experimental evaluation of thermal performance of two different finned latent heat storage systems. *Case Studies in Thermal Engineering*, 21:100675, 2020. doi: [10.1016/j.csite.2020.100675](https://doi.org/10.1016/j.csite.2020.100675).
- [36] L. Kalapala and J.K. Devanuri. Effect of orientation on thermal performance of a latent heat storage system equipped with annular fins – An experimental and numerical investigation. *Applied Thermal Engineering*, 183:116244, 2021. doi: [10.1016/j.applthermaleng.2020.116244](https://doi.org/10.1016/j.applthermaleng.2020.116244).

- [37] X. Yang, J. Guo, B. Yang, H. Cheng, P. Wei, and Y.L. He. Design of non-uniformly distributed annular fins for a shell-and-tube thermal energy storage unit. *Applied Energy*, 279:115772, 2020. doi: [10.1016/j.apenergy.2020.115772](https://doi.org/10.1016/j.apenergy.2020.115772).
- [38] Z. Elmaazouzi, I.A. Laasri, A. Gounni, M. El Alami, and E.G. Bennouna. Enhanced thermal performance of finned latent heat thermal energy storage system: fin parameters optimization. *Journal of Energy Storage*, 43:103116, 2021. doi: [10.1016/j.est.2021.103116](https://doi.org/10.1016/j.est.2021.103116).
- [39] S. Tiari, A. Hockins, and M. Mahdavi. Numerical study of a latent heat thermal energy storage system enhanced by varying fin configurations. *Case Studies in Thermal Engineering*, 25:100999, 2021. doi: [10.1016/j.csite.2021.100999](https://doi.org/10.1016/j.csite.2021.100999).
- [40] M. Sanchouli, S. Payan, A. Payan, and S.A. Nada. Investigation of the enhancing thermal performance of phase change material in a double-tube heat exchanger using grid annular fins. *Case Studies in Thermal Engineering*, 34:101986, 2022. doi: [10.1016/j.csite.2022.101986](https://doi.org/10.1016/j.csite.2022.101986).
- [41] Y. Zhu and Y. Qiu. Annular variable-spacing fin arrangement in latent heat storage system. *Journal of Energy Storage*, 50:104705, 2022. doi: [10.1016/j.est.2022.104705](https://doi.org/10.1016/j.est.2022.104705).
- [42] A.D. Brent, V.R. Voller, and K.J. Reid. Enthalpy-porosity technique for modeling convection-diffusion phase change: Application to the melting of a pure metal. *Numerical Heat Transfer*, 13(3):297–318, 1988. doi: [10.1080/10407788808913615](https://doi.org/10.1080/10407788808913615).
- [43] M. Longeon, A. Soupart, J.F. Fourmigué, A. Bruch, and P. Marty. Experimental and numerical study of annular PCM storage in the presence of natural convection. *Applied Energy*, 112:175–184, 2013. doi: [10.1016/j.apenergy.2013.06.007](https://doi.org/10.1016/j.apenergy.2013.06.007).
- [44] S.V. Patankar. *Numerical Heat Transfer and Fluid Flow*. CRC Press, 1980.
- [45] L. Pu, S. Zhang, L. Xu, and Y. Li. Thermal performance optimization and evaluation of a radial finned shell-and-tube latent heat thermal energy storage unit. *Applied Thermal Engineering*, 166:114753, 2020. doi: [10.1016/j.applthermaleng.2019.114753](https://doi.org/10.1016/j.applthermaleng.2019.114753).